$$\beta = -\frac{1}{\rho}\left(\frac{\partial \rho}{\partial T}\right)_x$$

ΔS = salinity difference, kg·m^{-3}

ΔT = temperature difference between two neighboring cells or between bulk and film, K

Δx = difference of liquid-phase mol fractions, dimensionless

$\Delta \rho$ = difference of liquid density for two neighboring cells or between bulk and film, kg·m^{-3}

κ = thermal diffusivity of LNG ($\kappa = k/\overline{C}\hat{C}_L$), 1.267×10^{-7} m^2·s^{-1}

λ_F = molar latent heat of vaporization of flash vapor, J·kgmol^{-1}

$\lambda(j)$ = latent heat of vaporization of species j at 99.82 K, J·kg^{-1}

μ = viscosity of LNG, kg·m^{-1}·s^{-1}

ν = kinematic viscosity of LNG, 2.787×10^{-7} m^2·s^{-1}

ρ_i = density of cell i liquid, kg·m^{-3}

$\overline{\rho}$ = averaged liquid density between two neighboring cells or between uppermost cell and the film, kg·m^{-3} [e.g., $\overline{\rho} = \frac{1}{2}(\rho_i + \rho_{i+1})$]

ρ_{BULK} = density of bulk liquid of the uppermost cell, kg·m^{-3}

ρ_{FILM} = density of liquid in the vaporizing film, kg·m^{-3}

LITERATURE CITED

Boyle, G. J., "Basic Data and Conversion Calculations for Use in the Measurement of Refrigerated Hydrocarbon Liquids," *J. Inst. Pet.*, **58**, 133 (May, 1972).

Chatterjee, N., and J. M. Geist, "The Effects of Stratification on Boil-off Rates in LNG Tanks," *Pipeline and Gas J.*, **199**, 40 (1972).

Chatterjee, N., and J. M. Geist, "Spontaneous Stratification in LNG Tanks Containing Nitrogen," Paper 76-WA/PID-6, ASME Winter Annual Meeting, New York (Dec. 5, 1976).

Germeles, A. E., "A Model for LNG Tank Rollover," *Advances in Cryogenic Engineering*, **21**, 326, K. D. Timmerhaus and D. H. Weitzel, eds., Plenum Press (1975).

Globe, S., and D. Dropkin, "Natural-Convection Heat Transfer in Liquids Confined by Two Horizontal Plates and Heated from Below," *Trans. ASME, J. Heat Trans.*, C81, 24 (1959).

Hashemi, H. T., and H. R. Wesson, "Cut LNG Storage Costs," *Hydrocarbon Processing*, 117 (Aug., 1971).

Hirata, M., S. Ohe, and K. Nagahama, "Computer Aided Data Book of Vapor-Liquid Equilibria," Kodansha Limited/Elsevier Scientific Publishing Co., Tokyo-New York (1975).

Huntley, S. C., "Temperature-Pressure-Time Relationships in a Closed Cryogenic Container," *Adv. in Cryogenic Eng.*, **3**, 342, Plenum Press (1957).

Huppert, H. E., "On the stability of a series of double-diffusive layers," *Deep-Sea Research*, **18**, 1005 (1971).

Joffe, J., M. Schroeder, and D. Zudkevitch, "Vapor-Liquid Equilibria with the Redlich-Kwong Equation of State," *AIChE J.*, **16**(3), 496 (1970).

Kato, M. W., K. Chung, and B. C.-Y. Lu, "Binary Interaction Coefficients of the Redlich-Kwong Equation of State," *Chem. Eng. Sci.*, **31**, 733 (1976).

Lamb, H., "Hydrodynamics," 6th ed., Article 232, Dover Publ. (1945).

McAdams, W. H., "Heat Transmission," 3rd ed., Chapter 7, McGraw-Hill Book Co., New York (1954).

Prausnitz, J. M., and P. L. Chueh, "Computer Calculations for High Pressure Vapor Liquid Equilibria," Prentice-Hall, Inc. (1968).

Sarsten, J. A., "LNG Stratification and Rollover," *Pipeline and Gas J.*, **199**, 37 (1972).

Soave, G., "Equilibrium Constants from a modified Redlich-Kwong equation of state," *Chem. Eng. Sci.*, **27**(6), 1197 (1972).

Turner, J. S., "The Coupled Turbulent Transports of Salt and Heat across a Sharp Density Interface," *Intl. J. Heat Mass Transfer*, **8**, 759 (1965).

Valencia-Chávez, J. A., "The Effect of Composition on the Boiling Rates of Liquefied Natural Gas for Confined Spills on Water," ScD Thesis, *Chem. Eng.*, MIT (1978).

Zudkevitch, D., and J. Joffe, "Correlation and Prediction of Vapor-Liquid Equilibria with the Redlich-Kwong Equation of State," *AIChE J.*, **16**(1), 112 (1970).

Supplementary material has been deposited as Document No. 04047 with the National Auxiliary Publications Service (NAPS), c/o Microfiche Publications, 214-13 Jamaica Avenue Queens Village, N.Y. 11428, and may be obtained for $4.00 for microfiche and $7.75 for photocopies.

Manuscript received March 23, 1981; revision received February 16, and accepted March 23, 1982.

Characteristics of a Transferred-Arc Plasma

M. T. MEHMETOĞLU and W. H. GAUVIN

McGill University
Montreal, Quebec, Canada

The basic characteristics of a transferred arc argon plasma were determined using a cathode assembly suitable for transferring the electric arc to a molten metal bath or to a cooled anode. They indicated that the sustained voltage depended strongly on the arc length and much less on current. The inlet gas velocity past the cathode tip was determined to be an important operating parameter, rather than the volumetric gas flowrate.

The measurement of the axial and radial profiles of temperature was effected with ±8% accuracy by a novel diagnostic technique. Temperatures up to 18,500 K were observed on the axis of the plasma column, near the cathode tip, and decayed in both radial and axial directions. A sweeping microprobe was used to measure the axial and radial profiles of velocity. Velocities up to 190 m/s were recorded. The presence of a relatively colder flow surrounding the plasma column was detected. Mass and energy balances performed by taking this flow into account agreed with the measured input rates.

SCOPE

The application of plasma technology to chemical and metallurgical processes has been receiving increasing attention in the last two decades. Not only does a thermal plasma as a heat source permit greatly increased rates of reaction in most processes of industrial interest, but it frequently allows reactions to occur which would not be feasible at the lower temperature

0001-1541-83-6605-0000-$2.00.

levels obtainable by conventional methods. A good example of this is the thermal decomposition of MoS_2 to yield molybdenum metal directly, with evolution of vapors of elemental sulfur which can be collected separately with no pollution problem. In addition, the plasma-forming gas can often be used as a reactant, for example, for oxidation (O_2, air), reduction (CO, H_2, CH_4), chlorination (Cl_2) or nitriding reactions (N_2).

To date, most of the research in this field has been devoted to exploring the technical feasibility of effecting the desired reactions under plasma conditions, rather than optimizing and controlling the plasma system so as to make it economically viable (Sayce, 1977; Gauvin et al., 1981). The latter is a consideration of the highest importance, in view of the high cost of electrical energy. As a consequence and although plasma generators capable of continuous operation at a power of several megawatts are commercially available, the use of plasma reactors on a commercial scale is limited to a few processes: the production of acetylene, that of titanium oxide, the dissociation of zircon sand, and smelting operations in steel making. Rykalin (1976), Sayce (1972, 1977), Hamblyn (1977), Aubreton and Fauchais (1978), and very recently Fauchais (1980) have reviewed the use of plasmas for high-temperature heterogeneous systems. From these reviews, it is the authors' contention that the transferred arc plasma in which an arc is struck between a cathode and a molten bath (acting as the anode) is often far more thermally efficient than the nontransferred arc plasma (for example, r.f. plasmas and d.c. jet plasmas).

All the energy supplied to the plasma system (less the small amount lost to cool the cathode) is present in the plasma column which is established between the cathode and the anode when an electric arc has been struck between the two electrodes. The length of this column may range between a few centimeters and up to a meter or more depending on the power. From a chemical engineering point of view, the temperature and velocity fields in the plasma column of a transferred arc are the most important parameters for the study, design and control of the plasma system, since they govern the amount of energy which will be radiated to the surroundings from the plasma column (and which must be utilized, for example, for heating the feed material) and the energy which will be transferred to the molten material acting as the anode, as well as the other lesser modes of heat transfer (e.g., by convection).

The objective of this study was, therefore, to characterize these parameters as a function of the operating variables which can be controlled in a transferred arc plasma system.

CONCLUSIONS AND SIGNIFICANCE

The basic characteristics of a transferred arc plasma and their variation with the operating parameters were studied experimentally. Argon was used as the plasma-forming gas. The plasma was operated between power levels of 8.4 and 38.5 kW. The current was varied between 150 and 350 amperes and the arc length between 4 and 8 cm. It was observed that the inlet velocity of the plasmagen gas past the cathode tip (calculated as the cold gas flow rate divided by the free annular nozzle area) was an important parameter and should be used instead of the volumetric gas flow rate alone, if the results are to be generalized.

The voltage characteristics under the major operating conditions showed that voltage depended strongly on the electrode separation and much less on the current and on the inlet gas velocity. The voltage gradient of the plasma column was calculated from the gradient of the linear portion of the voltage vs. electrode spacing graphs. The experimental measurements of the potential variation along the length of the column by means of probes confirmed the above approximations.

Calorimetric measurements were carried out to determine the fractions of the power supplied: (a) lost to the cathode tip and nozzle cooling; (b) dissipated to the cold surroundings by radiation from the plasma; and (c) released at the anode. The fraction of the power lost to the cathode and the nozzle was invariably small and almost constant with current and electrode separation. As the current was increased, substantial increase was observed in the amount of the power released at the anode. The electrode separation also had a considerable effect on the latter. Depending on the electrode separation the power radiated by the arc could be varied between 41% and 53%, independently of the current. The inlet gas velocity was found to decrease the cathode tip temperature by convective cooling.

The temperature measurements in the plasma column were effected with a novel electro-optical system capable of measuring the temperature profile of plasmas above 8,000 K with an accuracy of ±8%. The results indicated higher centerline temperatures near the cathode. Increasing the current and the inlet gas velocity both increased the temperature of the plasma. The validity of the LTE in the plasma was checked theoretically and its existence was confirmed. The maximum temperature measured in the work was 18,500 K for a 250-A arc with 4-cm electrode separation and 41-m/s inlet gas velocity.

A miniature, uncooled pitot tube connected to a high response-time differential pressure transducer was swept through the plasma to determine the plasma gas velocity distribution. Because of the low Reynolds number of the flow encountered under most of the plasma operating conditions, a correction for viscosity effects had to be included into the Bernoulli equation. The velocity profiles showed a strong decay in the radial direction, and a somewhat slower decay in the axial direction. The velocities tended to increase with increasing current and inlet gas velocities. When mass flow densities were calculated, existence of a relatively cold flow outside the boundaries of luminous column was discovered. It was observed that this flow was decreasing downstream which was taken as an indication of entrainment. The maximum axial velocity measured was 190 m/s near the cathode with an accuracy of ±7%.

Mass and energy balances computed at various axial distances for various operating conditions agreed with the input rates and thus confirmed the accuracy of the temperature and velocity measurements.

These findings are of significant importance for the design, control and optimization of plasma systems based on transferred arcs.

INTRODUCTION

The overall basic characteristics of a transferred-arc plasma have received little attention in the past. The work of Stojanoff (1966, 1968) in which a 3-cm long transferred arc was diagnosed for the purpose of obtaining the transport properties of argon plasmas is a notable exception. The scatter of the transport parameters obtained by this author and the large deviations from the theoretical values at high temperatures raise serious doubts about the accuracy of his temperature and velocity profiles, probably linked to the inaccuracy of his diagnostic techniques.

In a recent study, J. E. Fink (1980) has attempted to analyze, by means of a computer simulation, the complex situation existing immediately downstream from the tip of a fluid convective cathode in a transferred arc plasma system. Inclusion of the charge conservation equation and of a more comprehensive current density

expression gave the solution a considerable degree of generality. In view of the many assumptions made in the derivations, however, the results can only be used as first approximations at this time.

The diagnostic techniques used for plasmas show a considerable diversity. For temperature measurements, either insertion probes or optical methods, or a combination of both, have been used. The calorimetric probe is the most commonly used type of the first group and was mainly developed by Grey and coworkers (1962, 1965, 1968). The applicability of such techniques for transferred arc temperature measurements is restricted due to their low measurement range (below 10,000 K), their limited resolution and their sensitivity to the setting of the coolant rate. The optical techniques, of which the spectroscopic methods are the most important, suffer from the fact that the measurements are time consuming and that the data analysis (as in the Abel Inversion) require the assumption of circular symmetry of the plasma column (Lochte-Holtgreven, 1968). In addition, the spectroscopically-measured temperatures are inescapably weighted averages (Burns, 1964) that can often deviate considerably from simple averages and therefore yield spurious values. These limitations can be eliminated if spectroscopic principles are combined with probing techniques, as done by Stojanoff (1968).

For velocity measurements, again a variety of techniques can be used; however, the transient uncooled pitot tube seems to be the most appropriate for measurements in a transferred arc plasma, basically due to its good spatial resolution and simplicity. Following the recommendations of Sheer et al. (1969), a correction, called Barker correction (Barker, 1922), has to be made for viscosity effects at low Reynolds numbers.

In summary, the diagnostic techniques currently used for velocity and temperature measurement are lacking in simplicity and reliability. Therefore, the work reported in this paper represents an attempt to develop simple techniques for plasma diagnostics and to determine the basic plasma characteristics and their variations with operating variables in a transferred arc plasma.

EXPERIMENTAL

The apparatus used in the experimental work consisted of a power supply (maximum power 40 kW), a control console, and a transferred arc system including a cathode assembly, an anode assembly and a driving mechanism to adjust the interelectrode distance. A schematic drawing of the overall setup is given in Figure 1. Argon (purity 99.997%) was used as the plasmagen gas.

A cathode assembly suitable for operation in the transferred arc mode and for injection of fine particles, or of a secondary gas other than the main plasma-forming gas, was designed. The cathode assembly consisted essentially of a water-cooled conical thoriated tungsten cathode tip surrounded by a water cooled brass nozzle. The injection gas was fed through three equally-spaced feed tubes, each 0.4 cm in diameter. The angle of the injection channels and of the cathode tip was the same as that of the nozzle used. The plasma gas was forced to pass through a narrow shroud, the width of which could be adjusted by moving the cathode tip up or down. The nozzle directed this thin, high velocity layer of gas so that it impinged on the arc column in the region of the contraction zone. It was expected that with this configuration, the component of input gas momentum parallel to the arc axis exerted a stabilizing influence on the entire arc column. The thin layer of plasma gas was also intended to convectively cool the cathode tip and thus reduce the cooling requirements. The anode assembly consisted of a water cooled flat copper disc, 5.714 cm in diameter.

MEASUREMENT TECHNIQUES AND INSTRUMENTATION

Electrical and Calorimetric Characterizations

In the first part of the experimental work, the electrical characterization of the transferred arc plasma was carried out. For this purpose, the arc voltage was monitored as a function of various operating parameters.

The distribution of the voltage along the arc length with respect to the cathode was also measured. This was achieved by connecting a 0.1-mm tungsten wire to the positive end of an oscilloscope via a 100-kohm resistor. The negative terminal of the oscilloscope was connected to the cathode. The wire was then swept through the plasma, at various vertical positions, with a speed high enough to prevent thermal ablation of the wire. The wire velocity did not affect the results.

To obtain the fractions of the input power lost to the different parts of the equipment, the cathode, the nozzle and the anode were used as calorimeters.

Temperature Measurement Technique

A new electro-optical technique was developed for the measurement of plasma temperatures about 8,000 K. The basic prin-

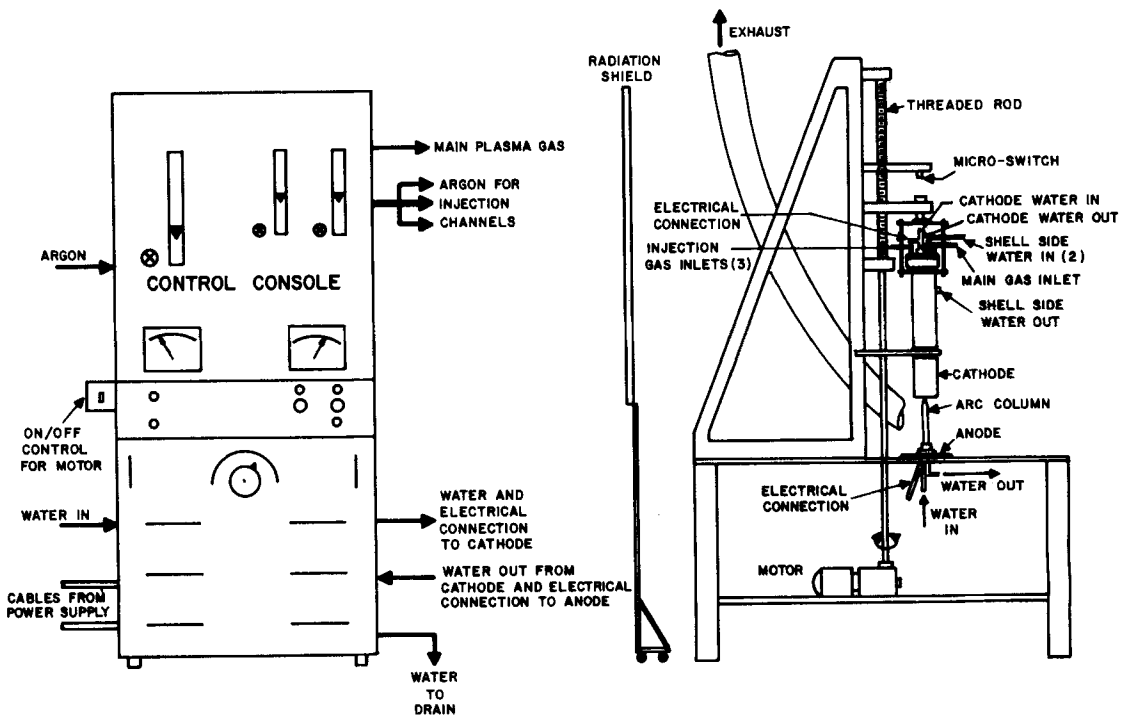

Figure 1. Schematic drawing of equipment.

ciple of this technique was to determine the total emission coefficients of the plasma at two wavelengths, as a function of radial position. The radial temperature distribution was then obtained by comparing the ratio of the measured emission coefficients with the theoretically-calculated values. A detailed description of this technique is given elsewhere (Mehmetoğlu et al., 1982).

Impact Pressure Measurement Technique

A dynamic pressure probe was developed to obtain direct flow field distributions in the transferred arc column. The probe involved in this work follows the design of Barkan and Whitman (1966). It consisted of a miniature stainless steel pitot tube (1.5875 mm OD, 0.508 mm ID, 3.75 cm long) swept through the column. The pitot tube was connected via teflon fittings to a pressure transducer which produced a signal proportional to the local dynamic pressure. The velocity and mass flow densities were then derived from the dynamic pressure with the aid of the Bernoulli equation corrected for viscous effects. The pressure transducer was a Celesco Model P109D miniature variable reluctance differential pressure transducer, with a sensitivity of <0.03 kPa, and was firmly attached on a mounting assembly which was driven by a linear motor. The transducer and the pitot tube were calibrated against an accurate alcohol manometer. It was ascertained that, at a traverse speed of 20 cm/s, the transient response of the system was satisfactory.

The final equation used to calculate the velocity, U, was:

$$1.1\Delta P_{\text{exp}} = \tfrac{1}{2}\rho U^2 + \tfrac{3}{2}\mu U/a \qquad (1)$$

in which the second term on the right represents the Barker (1922) viscosity correction. The factor 1.1 on the left accounts for a linear discrepancy observed in Barker's work. Following the results of Carleton (1970), the temperature used in the determination of viscosity and density was chosen to be that corresponding to the mean enthalpy of the pitot tube wall and free stream. Both μ and ρ were corrected for departures from the ideal gas law, using theoretically-derived relations between viscosity and compressibility versus temperature (Ahtye, 1965).

RESULTS AND DISCUSSION

Total Arc Voltage Analysis

Preliminary experiments were first carried out, using sheath gas only (that is, argon flowing through the annulus surrounding the cathode tip) to ascertain the effect on the voltage of the following variables: the applied current, I (150, 250, 350 A); the electrode separation, l(4, 6, 8, 10 cm); the argon volumetric flow rate, Q (14, 17, 20 L/min); the annular nozzle area, A (0.085, 0.07, 0.055 cm^2). A 60° nozzle (with the horizontal) was used. Typical results of such measurements are shown in Figure 2. It was, of course, realized that under these conditions considerable entrainment of ambient air into the plasma column would take place near the cathode tip due to magnetic pinching, or the Maecker effect.

A major finding of this part of the work was the observation that the gas flow rate and the annular nozzle area could be combined into a single parameter "the inlet gas velocity," which is the ratio of these two variables with the unit of m/s. This observation has very important implications for the design of commercial plasma reactors, since it should permit considerable savings by cutting down the volumetric flow rate of expensive plasmagen gas, as long as its velocity past the cathode is maintained.

To minimize or eliminate the effect of entrained air, these experiments were repeated with additional argon injection into the plasma column via the three injection channels in the cathode assembly, in addition, of course, to the sheath gas, as previously used. Two nozzle angles (60° and 45° with the horizontal) with the same nozzle diameter (0.381 cm) were used. The results of these experiments are shown as a factorial plot on Figure 3. Predictably, the values of the sustained arc voltage were lower than those previously

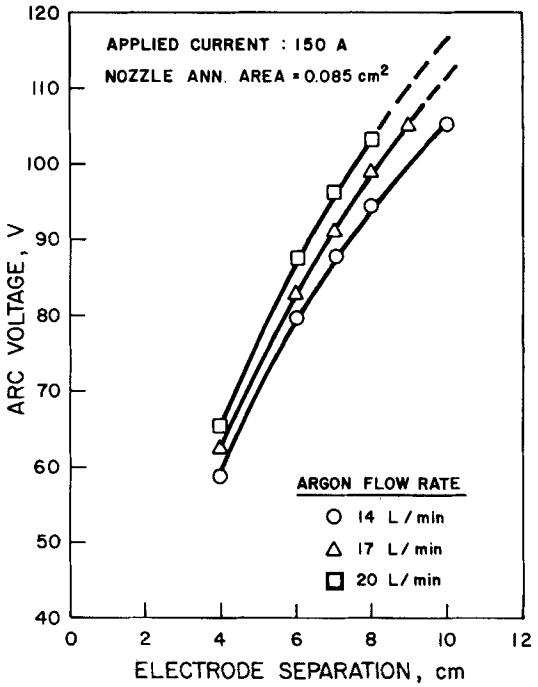

Figure 2. ARC voltage variation with electrode separation (low current, large area).

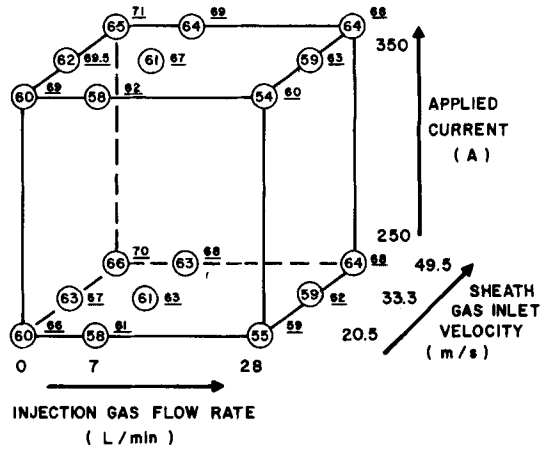

NOTES:
1. (V) VOLTAGE FOR 60° NOZZLE (SET III A)
2. V VOLTAGE FOR 45° NOZZLE (SET III B)

Figure 3. Experimental ARC voltage for various operating conditions (electrode separation: 4 cm). Circled figures indicate voltages for 60° nozzle; underlined smaller figures indicate voltages for 45° nozzle.

obtained in the presence of air entrainment, since the electric conductivity of pure argon is higher than that of air above 10,000 K (Ahtye, 1965; Devoto, 1967).

One important consequence of this observation is that an optimum condition could be found where increasing the injection gas flow rate will not lower the sustained voltage any more but, on the contrary, will increase it (the same effect of increasing sheath gas inlet velocity). At that point, the plasma was 100% argon plasma.

Finally, the effect of the nozzle angle can be observed from Figure 3. For all the conditions studied, lower voltages were recorded for 60° nozzles, which corresponded to a greater arc stability, as observed by Sheer et al. (1973). It was estimated that the accuracy of the voltage results was ±2 V.

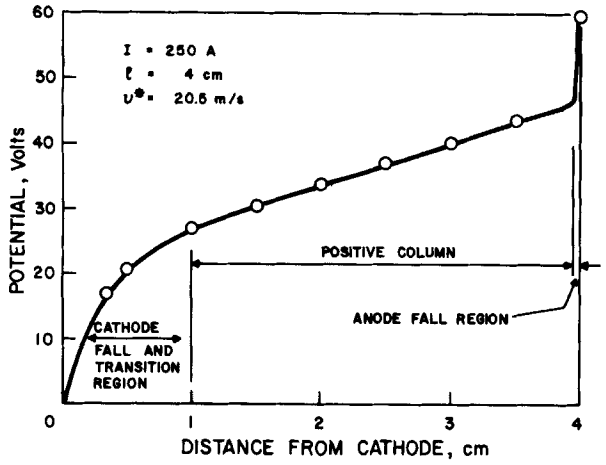

Figure 4. Axial potential distribution.

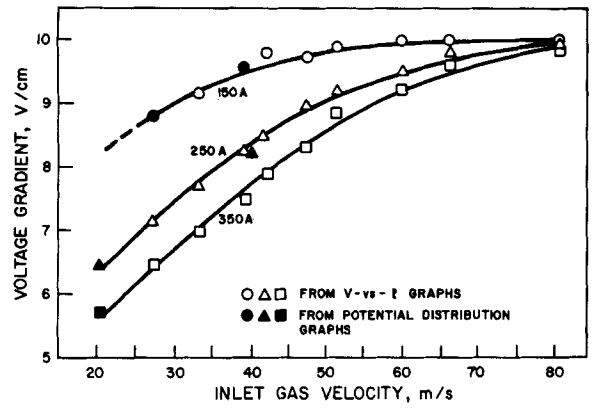

Figure 5. Variation of voltage gradient with inlet gas velocity and current.

Voltage Gradient Study

The determination of the voltage gradient is important since it reflects the energy content of the column much more realistically than the total arc voltage (which includes the electrode potential drops). The standard method for obtaining a voltage gradient is to measure the potential distribution along the arc length by means of a sweeping wire.

The axial potential distribution can also be calculated from the gradient of the linear portion of the graphs of the total arc voltage vs. electrode separation in the experiments previously described, for various currents and sheath gas inlet velocities, typical of which is Figure 4 (the thickness of the anode fall region in the latter is not accurate, but is known to be quite small). A comparison of the results obtained by the two methods is illustrated in Figure 5. The inherent assumption in the latter method is that the electrode spacing does not significantly influence the magnitude of the electrode falls. The results shown in Figure 5 indicate that the error due to this assumption is not very critical. The asymptotic behaviour of the curves for various currents at high inlet gas velocities is extremely interesting and was repeatedly confirmed experimentally for different operating conditions.

These results show that the column gradient increases with increasing inlet gas velocity, which may be explained by a greater loss of energy. The indirect proportionality between the voltage gradient and the applied current is obviously due to the increase in the electrical conductivity with increasing currents and, hence, temperatures.

Calorimetric Study

A large number of different heat transfer processes occur in a transferred arc system. A detailed analysis of these processes was the subject of another study carried out in this laboratory (Choi, 1981). In the present work, however, only the net amount of the heat released at the anode, at the cathode tip and at the nozzle was measured. Assuming that the convective losses from the plasma column to the ambient as well as the sensible energy loss to the exit gas were small, the heat radiated could be determined by difference, from the total arc power. The results of the calorimetric study are shown in Table 1.

Heat Transfer to Anode

It was observed that the anode heat fluxes increased with increasing current, increasing inlet gas velocity and also increasing electrode separation, in accord with the extensive anode studies performed by Pfender and coworkers (Smith and Pfender, 1976; Pfender, 1978; Liu and Pfender, 1979; Johnson and Pfender, 1979). Although there was an increase in the absolute value of the heat transferred to the anode with increasing length, when the percentage of the arc energy transferred was considered, a steady decrease (from 44% at 4 cm to 38% at 8 cm) was observed. It is evident that the increase in the radiation loss was responsible for this decrease in the fraction of arc energy transferred to the anode.

Arc Radiation

As expected, arc radiation increased with the applied current. This is in complete agreement with several previous workers. The

TABLE 1. CALORIMETRIC RESULTS

	Cathode Tip		Nozzle		Anode		Arc Power	Radiation	
v^*	P_c	%	P_n	%	P_a	%	P	$P-(P_c+P_n+P_a)$	%
m/s	kW		kW		kW		kW	kW	
	l = 4 cm							I = 250 A	
16.65	0.45	3.5	1.16	9.1	5.67	44.5	12.75	5.47	42.9
33.30	0.43	3.2	1.19	9.1	5.88	44.8	13.13	5.63	42.9
49.95	0.41	3.0	1.28	9.4	6.37	46.8	13.62	5.56	40.8
	l = 4 cm							I = 350 A	
16.65	0.67	3.6	1.62	8.7	8.03	43.3	18.55	8.23	44.4
33.30	0.65	3.4	1.75	9.3	8.20	43.8	18.73	8.13	43.1
49.95	0.55	2.8	1.79	9.2	8.20	42.6	19.25	8.71	45.4
	v^* = 33.30 m/s							I = 350 A	
ℓ	P_c	%	P_n	%	P_a	%	P	$P-(P_c+P_n+P_a)$	%
cm	kW		kW		kW		kW	kW	
6	0.66	2.6	1.90	7.8	10.22	41.7	24.50	11.72	47.9
8	0.66	2.3	1.95	6.7	10.98	37.8	29.05	15.46	53.2

inlet gas velocity, on the other hand, was observed to have less influence on the amount of heat lost by radiation. It should be emphasized that the radiation terms shown in Table 1 also contain convective contributions.

Heat Transfer to Cathode Tip and Nozzle

As in the case of the anode, heat transfer to the cathode tip increased with current. This is obviously due to the increased current density which is the major contributor to the heat transfer to the cathode tip (Guile, 1971). The increase in the heat transferred to the nozzle with increasing current was lower than in the case of the cathode tip. In this case, the heat transfer was basically due to radiation and hence the percentage change in the heat transfer followed that of radiation with current.

There was a small but persistent decrease in the cathode tip heat flux with increasing inlet gas velocity. This change, however, was not close to the experimental error predicted, especially for low current cases. Direct measurements of the cathode tip temperatures with an optical pyrometer confirmed these findings.

Plasma Temperature Analysis

As already stated, the details of the novel technique of measurement which was used in this section of the study are presented elsewhere (Mehmetoğlu et al., 1982). Suffice it to say that considerable care was taken in its development, and that its estimated accuracy (±8%) compares favourably with the conventional spectroscopic methods.

The plasma temperature was obtained at different vertical locations with 1 cm separation, except for the uppermost position which was 0.5 cm away from the cathode tip. No measurements were attempted for locations closer than 1 cm from the anode since it is well established that LTE does not hold close to the electrodes (Eddy et al., 1973). A typical isothermal contour is shown in Figure 6, for operation with and without injection gas. The axial centerline temperature distributions for the various conditions used are plotted in Figure 7. Finally, to demonstrate the effect of the operating parameters on temperature distribution, sample profiles (obtained 3 cm away from the anode) are plotted in Figure 8.

Examination of these curves shows that the axial temperatures increase near the cathode as the inlet gas velocity increases. This effect is considered to be due to the compression of the column exerted by the radial component of the fluid momentum as it enters the column. It is interesting to note the rather flat portion of the axial temperature distribution for $0.5 < z < 1.0$ cm, in Figure 7. It probably represents the section of the contraction zone where most of the gas is entering the column. The two previous investigators who used similar cathode designs (Sheer et al., 1973; Stojanoff, 1968) also displayed similar distributions near the cathode,

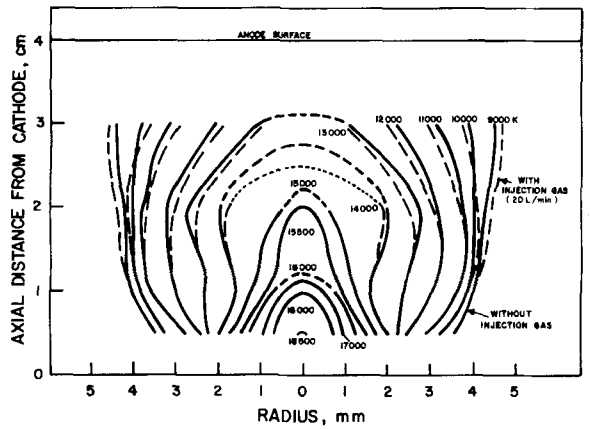

Figure 6. Isothermal contours of the plasma for $\ell = 4$ cm, $I = 250$ A, $v^* = 41$ m/s, and $q = 20.0$ L/min.

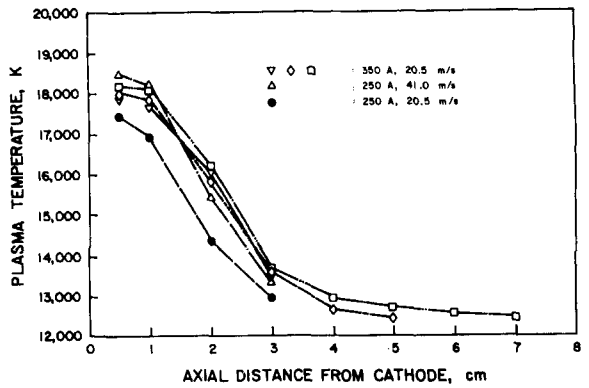

Figure 7. Axial centerline temperature distribution in plasma column.

as shown in Figure 7. The theoretical calculations of Fink (1980) also predict this behaviour.

The plasma temperature increases as the applied current increases. As can be seen from the axial temperature distribution, the magnitude of this increase does not change along the arc length. This effect had already been predicted by the calorimetric and photographic studies. Although the voltage gradient decreases with increasing current, the increase in the current density more than compensates for this decrease.

The comparison of the axial distributions shown in Figure 7 for the 4, 6 and 8 cm columns shows that identical temperatures are obtained for the initial portion of the column included in these cases. The fact that the decay in axial temperature decreases considerably beyond a distance of 3 cm away from the cathode for the 6- and 8-cm arc lengths suggests that the phenomenon which is responsible for the loss of energy in the initial part of the plasma ceases to be important after 3 cm. Considering that radiative heat losses constitute a large percentage of the overall heat losses from the plasma column, the low temperatures encountered around $z = 3$ cm results in lower radiative heat losses and thus slower decay. This cause-effect relationship sets in for the rest of the plasma column. The results of Choi (1981), who measured arc radiation as a function of arc length for transferred-arc plasma under similar conditions, also indicate a sharp change in the percentage of the arc energy lost by radiation beyond a 3-cm electrode separation. To complete this discussion, it must be stated that other factors such as the decreasing effect of the cathode jet are also probably responsible for the sudden drop in the axial temperature upstream of 3 cm.

Finally, the effect of varying the nozzle angle can be observed from Figure 8. The position of the 9,000 K isotherms does not

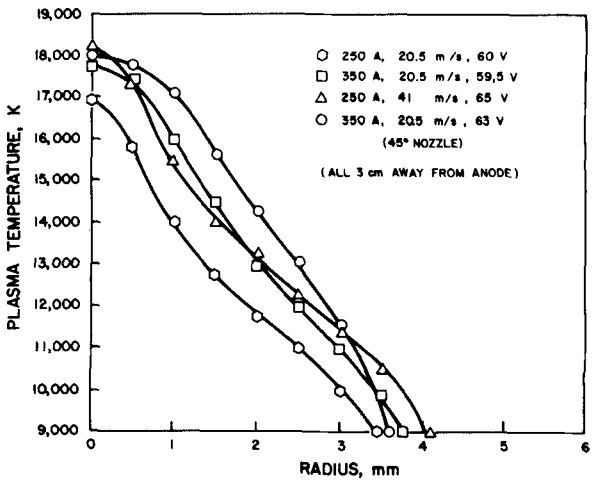

Figure 8. Radial distribution of temperature in plasma column. (at 3 cm away from anode for 4 cm total length, all symbols, except circles, are for 60° nozzle).

change between the two conditions at 350 A (Square symbols for 60° and circles for 45° nozzle). Higher temperatures result for the 45° nozzle near the cathode. The magnitude of this difference decreases downstream from the cathode. The effect of the nozzle geometry on the energy content of the plasma in the neighbourhood of the cathode can be attributed to the change in the electrode fall potential.

It should be mentioned that the above temperature distributions are based on the assumption of local thermal equilibrium (LTE) in the plasma. This assumption has been experimentally tested and found fully justified for transferred arc plasmas generated under similar conditions and with similar cathode design as used in this work (Stojanoff, 1968; Sheer et al., 1973). Busz and Finkelnburg (1955) obtained the following criterion for thermal equilibrium:

$$(T_e - T_g)/T = (M(e\lambda_e E)^2/4m(3kT/2)^2 \ll 1 \qquad (2)$$

where T_e, T_g are the temperatures of the electrons and heavy particles, respectively, E is the applied electric field strength, M and m are the masses of the atoms and electrons, respectively, and λ_e is the electron mean free-path length. Using the value of λ_e calculated by Olsen (1962), the measured temperatures and derived E, $(T_e - T_g)/T$ were calculated to be (at the centre of the arc) 0.006 near the cathode and 0.01 near the anode, for 250 A and 20.5 m/s. In the light of this test, it can be claimed that the assumption of LTE throughout the measurement range of this work is very good.

A more restrictive condition for LTE pertains to the gradients in temperature along the radial coordinate in the arc. The perturbation of equilibrium may be considered small if the temperature difference in one mean-free path is small compared with the temperature itself (Olsen, 1962);

$$\lambda_e \text{ grad } T/T \ll 1 \qquad (3)$$

The maximum temperature gradient measured in the arc is around 10^5 K per cm. Since λ_e is of the order of 10^{-4} cm with temperatures greater than 10^4 K, the condition in the above equation is well satisfied, except possibly in the regions close to the electrodes, which is outside the scope of this study.

VELOCITY STUDY

Method of Data Resolution

The values of the impact pressures obtained from the continuous impact pressure profile together with the measured temperatures at the same radial positions permitted calculation of the plasma velocities at these points using Eq. 1. The calculation was performed by a minicomputer. Since the viscosity and density in Eq. 1 must be evaluated at the reference temperature, the probe wall temperature was estimated to be 400 K. The insensitivity of the reference temperature to the wall temperature justifies this choice. This particular wall temperature was chosen based on thermocouple measurements of the temperature of the probe after it completed a traverse. The computations were made at 18 equally spaced positions along the diametrical pressure profile.

Results

A typical velocity contour is shown in Figure 9, for conditions identical with those used for Figure 6. Figure 10 shows the axial distribution of the centreline velocity and in Figure 11, a sample of the radial velocity distributions is given, for the position 3 cm away from the anode, to assist in the discussions. Finally, Figure 12 contains a set of typical mass flow density distribution curves, for various distances from the anode. The limiting data points on the velocity profiles are determined by the limiting points on the temperature profiles which, in turn, are established by the luminous diameters of the column. Beyond these positions, impact pressures could be measured, but temperatures could not.

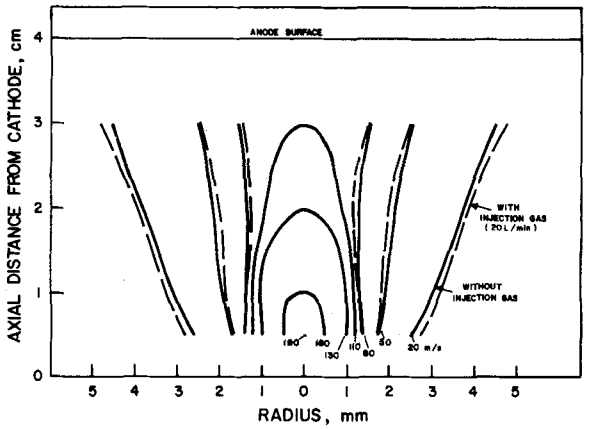

Figure 9. Constant velocity contours of the plasma column for ℓ = 4 cm, I = 250 A, v^* = 41 m/s, and q = 0 L/min and q = 20 L/min.

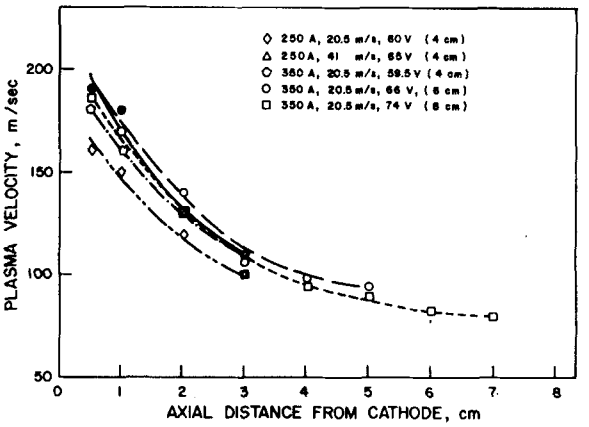

Figure 10. Axial centerline velocity distribution in plasma column.

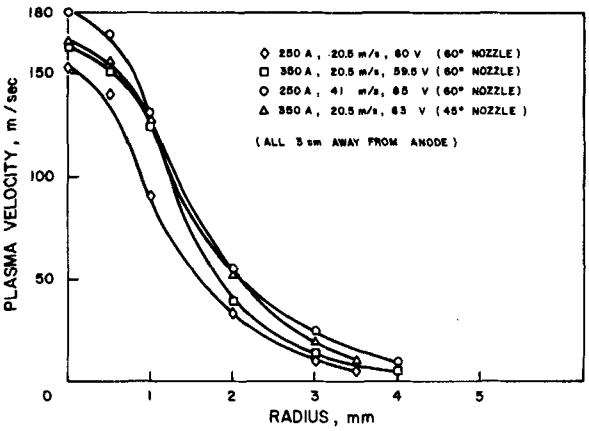

Figure 11. Radial distribution of velocity in plasma column (at 3 cm away from anode for 4-cm total length).

It can be seen that, as in the case of temperatures, the velocity profiles are symmetric. The decay of the centreline velocity with the axial distance from the cathode is observed to be faster than that of the centreline temperature.

Examination of these figures indicates that both the inlet gas velocity and the applied current increase centre velocities. However, when the radial distributions are compared (Figure 10), it can be seen that, towards the edges of the column, the effect of the applied current ceases to be significant. Since Reynolds numbers are quite low near the edges (around one compared to around 90 at the axis), the viscosity corrections are much more important; however, because the viscosity does not vary significantly with temperature below 10,000 K, it is normal that the applied current

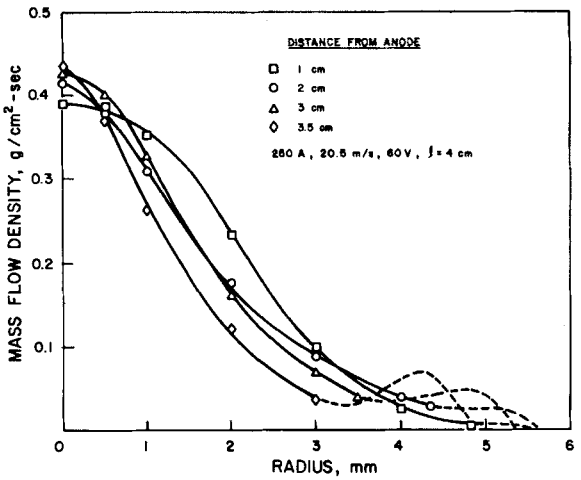

Figure 12. Radial distribution of mass flow density for plasma column (ℓ = 4cm, I = 250 A, v^* = 20.5 m/s).

(which influences the temperature distribution near the edges) does not influence velocity profiles in these regions.

While the nozzle angle does not influence the axial distribution, it does have an effect on the radial velocity distribution in the form of a slower decay for 45° nozzle. This is predictable from the temperature profiles and is considered to be an important feature in favour of the selection of a 45° nozzle for industrial applications.

Since the column is cooling and increasing in density as the anode is approached, the product of density and velocity, or momentum, is of interest. Figure 12 shows a typical plot of the mass flow density ($\dot{m}$) versus radial distance. When the distributions of impact pressure were examined, it was observed that there existed a relatively cold gas flow outside the luminous boundaries of the column. The mass flow density distribution calculated for this flow is also shown in Figure 12, as dashed lines. The temperature data used outside the luminous column were obtained by extrapolation from the temperature distributions inside the column and are therefore subject to considerable error. The curves are extended into this outer region to show qualitatively the changes in flow pattern at various axial positions. The amount of gas that flows outside the column seems to decrease downstream. This undoubtedly indicates entrainment of the surrounding flow. It is interesting to note that although the presence of this flow can be deduced from their results, neither of the two investigators who worked with an annular nozzle orifice around a cathode (Stojanoff, 1968; Sheer et al., 1973) realized this occurrence. The theories of classical jet entrainment are found wholly inadequate to account for this change of entrainment with axial distance. For the experimental conditions reported, the maximum uncertainty in the calculated velocity ranges from ±7.0% in the vicinity of the centreline to ±20.0% near the edges.

Mass and Energy Balances

By using the experimentally-measured values of the temperature and velocity, mass and energy balances could be made for the plasma flows. The mass flow rate M and the energy flow rate H are calculated from:

$$M = \int_0^{2\pi} \int_0^R \dot{m}(r) r dr d\theta \tag{4}$$

and

$$H = \int_0^{2\pi} \int_0^R \dot{m}(r) h(r) r dr d\theta \tag{5}$$

where $\dot{m}$ is the mass flow density and h is the specific enthalpy.

A minicomputer was used to perform the calculations. Ahtye's (1965) data for compressibility and enthalpy were fitted numerically, and the required integrations across the plasma column were performed by using Simpson's rule. The integrations were first performed only out to the luminous profile of the plasma column. The integration was then carried out to the fringes of the impact pressure profiles, using the extrapolated temperature values. The results of the mass and energy balances showed that the agreement between the measured rates and the calculated values were satisfactory, with an average error of ±15% for the mass flow and ±20% for the energy flow.

NOTATION

a = inside radius of the pitot tube
A = annular nozzle area
E = voltage gradient
h = specific enthalpy
H = energy flow rate
H = applied current
ℓ = electrode separation
$\dot{m}$ = mass flow density
m = mass of electron
M = mass flow rate—also mass of atom in Eq. 2
P = pressure
q = injection gas flow rate
Q = sheath gas volumetric flow rate
r = radial position
R = radius of plasma
T = temperature
U = gas velocity
V = voltage
v^* = inlet gas velocity
z = axial distance from cathode

Greek Letters

λ = length of mean free path
ρ = gas density
μ = viscosity of the plasma
θ = angle

Subscripts

e = electrons
g = gas (heavy particles)

ACKNOWLEDGMENT

The authors gratefully acknowledge the financial support of the Quebec Ministry of Education in the form of a grant for an Action Concertée on plasma technology.

LITERATURE CITED

Ahtye, W. F., "A Critical Evaluation of Methods for Calculating Transport Coefficients of Partially and Fully Ionized Gases," NASA TN D-2611, Washington, DC (1965).

Aubreton, J., and P. Fauchais, "Les Fours à Plasma," *Rev. Gen. Therm. Fr.*, No. 200-201, 681 (Aug.-Sept., 1978).

Barkan, P., and A. M. Whitman, "Stagnation Pressure Measurement in a Current Carrying Plasma," *AIAA Technical Notes*, **4**, 9 (1966).

Barker, M., "On the Use of Very Small Pitot Tubes for Measuring Wind Velocity," *Proc. Roy. Soc. of London*, **101**, 435 (1922).

Burns, J., "Research on Effects of Arc Fluctuations on Spectroscopically Determined Temperatures in Arc Plasmas," Air Force Materials Lab., Res. and Tech. Div., Air Force System Command, TDR ML-TDR-64-243 (1964).

Busz-Peuckert, G., and W. Finkelnburg, "The Anode Mechanism of the Thermal Argon Arc," *Z. für Physik*, **140**, 540 (1956).

Carleton, F. E., "Flow Patterns in a Confined Plasma Jet," Ph.D. Thesis, University of Michigan (1970).

Choi, H. K., "Energy Distribution and Heat Transfer in an Argon Transferred-Arc Reactor," Ph.D. Thesis, McGill University (1981).
Devoto, R. S., "Transport Coefficients of Partially Ionized Argon," *The Physics of Fluids*, **10**, (2), 354 (1967).
Eddy, T. L., E. Pfender, and E. R. G. Eckert, "Spectroscopic Mapping of the Nonequilibrium Between Electron and Excitation Temperatures in a 1 Atm Helium Arc," *IEEE Trans. on Plasma Science*, **PS-1**, (4), 31 (1973).
Fauchais, P., "Utilisation Industrielle Actuelle et Potentielle des Plasmas," *Revue Phys. App.*, **15**, 1281 (1980).
Fink, J. E., "Theory and Computation of the Characteristics of the Thermal Electrical Plasma Arc for Chemical Engineering Applications," *Chem. Eng. Commun.*, **5**, 37 (1980).
Gauvin, W. H., G. R. Kubanek, and G. Irons, "The Plasma Production of Ferromolybdenum—Process Development and Economics," *J. of Metals*, 42 (Jan., 1981).
Grey, J., P. F. Jacobs, and M. P. Sherman, "Calorimetric Probe for the Measurement of Extremely High Temperatures," *Rev. Sci. Instrum.*, **33**, (7), 738 (1962).
Grey, J., "Thermodynamic Methods of High-Temperature Measurement," *ISA Trans.*, **4**, 102 (1965).
Grey, J., "Proposed Method for Measuring Gas Enthalpy using Calorimetric Probes," ASTM, Committee E-21 on Space Simulation (1968).
Guile, A. E., "Arc-Electrode Phenomena," *IEEE Reviews*, **118**, 1131 (1971).
Hamblyn, S. M. L., "A Review of Applications of Plasma Technology with Particular Reference to Ferro-Alloy Production," National Inst. for Metallurgy, Report No. 1895 (1977).
Johnson, D. C., and E. Pfender, "Modelling and Measurement of the Initial Anode Heat Fluxes in Pulsed High Current Arcs," *IEEE Trans. on Plasma Sci.*, **PS-7**, (1), 44 (1979).
Liu, C. H., and E. Pfender, "Heat Transfer in the Anode Region of High Intensity Arcs," *Studies in Heat Transfer*, A Festschrift for E. R. G. Eckert, Hemisphere Publ. Corp., Washington (1979).
Lochte-Holtgreven, W., *Plasma Diagnostics*, North-Holland Publ. Co., Amsterdam (1968).
Mehmetoğlu, M. T., F. Kitzinger, and W. H. Gauvin, "A Novel Technique of Plasma Temperature Measurement," *Rev. Scient. Instrum.*, **53**, No. 3, 285–293 (1982).
Olsen, H. N., "Determination of Properties of an Optically Thin Ar Plasma," *Temperature: Its Measurement and Control in Science*, **3**, 593 (1962).
Rykalin, N. N., "Plasma Engineering in Metallurgy and Inorganic Materials Technology," *Pure and Appl. Chem.*, **48**, 179 (1976).
Sayce, I. G., and B. Selton, "Special Ceramics," ed., P. Popper, British Ceramic Research Assoc., Stoke-on-Trent, 157 (1972).
Sayce, I. G., "Some Applications of Thermal Plasmas to Material Processing," paper 107, Section 4A, World Electrotechnical Congress, Moscow (July, 1977).
Sheer, C., S. Korman, C. G. Stojanoff, and P. S. Tschang, "Diagnostic Study of the Fluid Transpiration Arc," Mechanical Div., Air Force Office of Sci. Res., AFOSR 70-0195 TR (1969).
Sheer, C., S. Korman, and S. F. Kang, "Investigation of Convective Arcs for the Simulation of Re-entry Aerodynamic Heating," Aeromechanics Div., Air Force Office of Sci. Res. (1973).
Smith, J. L., and E. Pfender, "Determination of Local Anode Heat Fluxes in High Intensity Thermal Arcs," *IEEE Trans. on PAS*, **PAS-95**, (2), 704 (1976).
Stojanoff, C. G., "A Transient Fiber Optics Probe for Space Resolved Diagnostics of Dense Plasmas," *AIAAJ*, **4**, (10), 1766 (1966).
Stojanoff, C. G., "Characteristics of an Axially Flow Stabilized Arc and Its Application to the Determination of Transport Properties," Ph.D. Thesis, Stuttgart University, (in German) (1968).
Wilkinson, J. B., and D. R. Milner, "Heat Transfer from Arcs," *Brit. Welding*, 115 (1960).

Manuscript received May 13, 1981; revision received March 9, and accepted March 23, 1982.

Turbulent Velocity Fluctuations That Control Mass Transfer to a Solid Boundary

J. A. CAMPBELL and T. J. HANRATTY

University of Illinois Urbana, IL 61801

The relation between the velocity and concentration fields for a fully developed turbulent flow which transfers mass to a pipe wall at large Schmidt numbers has been studied. Measurements of the fluctuations of the concentration gradient and the velocity gradient were obtained simultaneously at multiple locations on the wall. Spatial scales were calculated for the low frequency velocity fluctuations by passing the measured signals through low-pass filters. These scales are the same size as the scales of the concentration fluctuations. This result provides additional support for the notion that mass transfer to a boundary at high Schmidt numbers is controlled by low frequency velocity fluctuations which contain only a small fraction of the total turbulent energy.

SCOPE

A recent analysis by Campbell and Hanratty (1981a) using the linearized form of the mass balance equation for a turbulent flow shows that the magnitude of the Reynolds transport term is controlled by low frequency velocity fluctuations containing a small fraction of the total turbulent energy. The work described in this paper was carried out to see whether this interpretation is consistent with measurements of the scale of the turbulence and whether such low frequency velocity fluctuations are universal properties of the turbulence.

The structure of the velocity field close to a wall was studied by measuring the transverse component of the fluctuating velocity gradient simultaneously at multiple locations on the wall. By low-pass filtering the signals from these probes it is possible to compare the spatial scale of the low frequency velocity gradient fluctuations with the spatial scale of the full signal and with the spatial scale of the concentration fluctuations. By examining the measurements of the mass transfer fluctuations in different systems, it is possible to determine whether these fluctuations are strongly dependent on the design of the flow system.